International Journal of Biological Macromolecules 220 (2022) 472–481

Contents lists available at ScienceDirect

International Journal of Biological Macromolecules

journal homepage: www.elsevier.com/locate/ijbiomac

Lignin-based non-crosslinked nanocarriers: A promising delivery system of pesticide for development of sustainable agriculture

Wenlong Liang [a,c,1], Jiadong Zhang [a,1], Frederik R. Wurm [c], Rong Wang [d], Jingli Cheng [a], Zhengang Xie [a], Xianbin Li [b,*], Jinhao Zhao [a,*]

[a] Key Laboratory of Biology of Crop Pathogens and Insects of Zhejiang Province, Ministry of Agriculture Key Lab of Molecular Biology of Crop Pathogens and Insects, Zhejiang University, Hangzhou 310058, PR China
[b] Institute for the Control of Agrochemicals, Ministry of Agriculture, Beijing 100125, PR China
[c] Sustainable Polymer Chemistry, Department of Molecules and Materials, MESA+ Institute for Nanotechnology, Faculty of Science and Technology, Universiteit Twente, PO Box 217, 7500 AE Enschede, the Netherlands
[d] Economic Specialty Technology Extension Center, Lanxi 321100, PR China

ARTICLE INFO

Keywords:
Lignin
Sustainable agriculture
Nanopesticide
Crop protection
Controlled release

ABSTRACT

Lignin sulfonate (LS), a waste material from the paper pulping, was modified with benzoic anhydride to obtain benzoylated lignin sulfonates of adjustable hydrophilicity (BLS). When BLS was combined with difenoconazole (Di), a broad-spectrum fungicide, lignin-based, non-crosslinked nanoparticles were obtained either by solvent exchange or solvent evaporation. When a mass ratio of 1:5 LS: benzoic anhydride was used, the Di release from Di@BLS$_5$ after 1248 h was *ca.* 74 %, while a commercial difenoconazole microemulsion (Di ME) reached 100 % already after 96 h, proving the sustained release from the lignin nanocarriers. The formulation of Di in lignin-based nanocarriers also improved the UV stability and the foliar retention of Di compared to the commercial formulation of the fungicide. Bioactivity assay showed that Di@BLS$_5$ exhibited high activities and duration against strawberry anthracnose (*Colletotrichum gloeosporioides*). Overall, the construction of fungicide delivery nano-platform using BLS *via* a simple non-crosslinked approach is a novel and promising way to develop new formulations for nanopesticide and the development of sustainable agriculture.

1. Introduction

The world population has been increasing rapidly over the last decades. The United Nations forecasts that, as a median assumption, the population will reach 9.7 billion by mid-century and 11.2 billion by the end of the century [1]. It is estimated that food production will need to increase by about 70 % by 2050 and double or triple by 2100 [2]. Agricultural productions, the primary source of food, have increased food production over the years through the extensive use of agrochemicals, especially pesticides [3]. More than 4 million tons of pesticides are used each year to protect crops worldwide [4]. However, indiscriminate overuse of conventional pesticide formulations leads to high pesticide residues, environmental pollution, destruction of ecosystems and increased soil pollution, and pesticide resistance [5–7]. These severe damages are due not only to the inefficiency of pesticides but also to the heavy use of organic solvents and surfactants in conventional formulations [8]. In view of concerns about ineffective agrichemical delivery of agrochemicals and better development of sustainable agriculture, developing a new water-based, environmentally friendly, and effective pesticide delivery system becomes necessary [9,10].

Here, we present a novel, approach to construct lignin-based nanocarriers without chemical crosslinking for the sustained release of a fungicide with improved leaf-adhesion. Nowadays, with the rapid development of nanotechnology in different fields, nanotechnology offers a potential approach for better development of sustainable agriculture [11]. Compared with conventional pesticide formulations, the construction of nanocarriers showed superior performance in water-dispersible, permeability, duration, and efficacy [12,13]. Accordingly, various types of inorganic such as zinc oxide [14], metal-organic frameworks [15], and calcium carbonate [16], or synthetic polymers [17], biobased chitosan [18], and cellulose [19,20] have been used in

* Corresponding authors.
E-mail addresses: lixianbin@agri.gov.cn (X. Li), jinhaozhao@zju.edu.cn (J. Zhao).
[1] W. Liang and J. Zhang contributed equally to this work.

https://doi.org/10.1016/j.ijbiomac.2022.08.103
Received 28 June 2022; Received in revised form 9 August 2022; Accepted 15 August 2022
Available online 17 August 2022

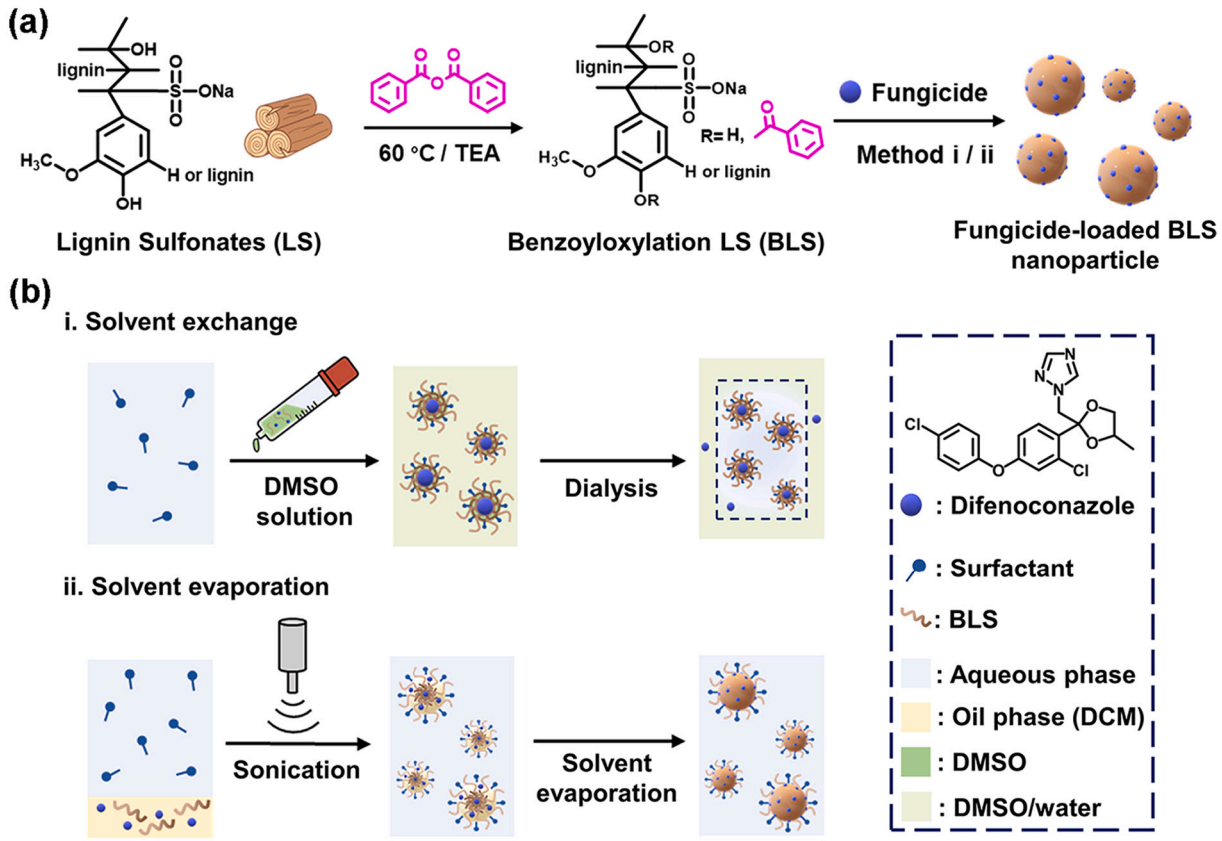

Scheme 1. (a) Synthesis of benzoyloxylation lignin sulfonates and (b) preparation of difenoconazole-loaded lignin-based nanocarriers by solvent exchange or solvent evaporation.

the construction of pesticide nanocarriers. However, pesticide formulation as an agricultural input, these nanocarriers will also leak into the environment with pesticides in agricultural production. Nondegradable inorganic nanoparticles and organic microplastics will remain in the environment for a long time and then accumulate in the food chains/webs, posing a potential risk to non-target organisms [21–23]. Although chitosan and cellulose are natural biodegradable polymers, their extensive use as pesticide nanocarriers is limited due to their insolubility in most organic solvents, high viscosity, and high cost for agricultural production [24,25]. Hence, a low-cost, biodegradable, easily functionalized material is desirable for delivering pesticides.

As the second most abundant renewable polymer in nature, lignin is one of the main components of wood and can be obtained from the by-products of pulping and paper-making industry [26,27]. In recent years, lignin and its modified derivatives have been favored as a sustainable materials in drug delivery [28], detection [29], especially in pesticide formulations due to its low cost, biodegradability, biocompatibility, and UV absorbance, which can improve the effective utilization of pesticide and reduce the potential risk of conventional pesticide formulation to the environment [30]. Currently, the most common preparation method of pesticide lignin nanocarriers is to form nanocapsule or micelles by interfacial crosslinking or self-assembly [31–33]. Lignin nanocapsule with a core-shell structure generally uses a hydrophobic organic solvent (xylene, toluene) as the core, and the lignin after interface crosslinking by adding crosslinking agent (diisocyanate) as the shell [31,34]. However, added organic solvents and diisocyanate with high reactivity may also have potential risks to the environment and undergo unwanted side reactions with various cargo molecules. Besides, another disadvantage of nanocapsule is that it may be easier to collapse, resulting in burst release of the encapsulated active component and then losing the duration [35]. For pesticide micelles, or pesticide microemulsions, the individual molecules or unimers that make up the micelle are in a dynamic equilibrium with the unimers in bulk, making it possible for micelles' size to change under certain conditions [36]. For example, when pesticide micelles are sprayed on crops, pesticide particles tend to aggregate into large sizes on the surface of the leaves rather than disperse singly in nanoscale, which will significantly reduce the effective rate of pesticides [15]. Hence, developing a simpler, environmentally friendly, particle size stable, and water-based lignin pesticide nanocarrier is an effective means to promote sustainable agriculture.

In this study, in order to prepare pesticide nanocarriers with better dispersion in water, the lignin sulfonates (LS) with negative charge were used as raw material. However, due to the strong hydrophilicity of LS, it is not conducive to formation of nanoparticles in water. Therefore, benzoic acid, a common and relative safe agricultural and food preservative, as a lipophilic group, was used to esterify with LS to obtain benzoic acid esterified lignin sulfonates (BLS) of adjustable hydrophobicity. According to whether BLS with different degrees of substitution can dissolve in DCM as the standard to judge the amphiphilicity of BLS, the fungicide was loaded through two methods to firstly obtain fungicide-loaded BLS nanoparticles (Scheme 1). In addition, the optimal nanoparticles with the best formulation stability were selected, and their release performance, photostability, *in vitro* or *in vivo* biological activity against model pathogen strawberry anthracnose (*Colletotrichum gloeosporioides*), and foliar retention and distribution on the cucumber leaves and peanut leaves were investigated in detail to reveal the potential application prospect of the BLS nanocarriers for pesticide delivery.

2. Experimental section

2.1. Materials and chemicals

Lithium chloride anhydrous (99 %) was purchased from Shanghai Macklin Biochemical Co., Ltd. (China). Difenoconazole (96 %) was

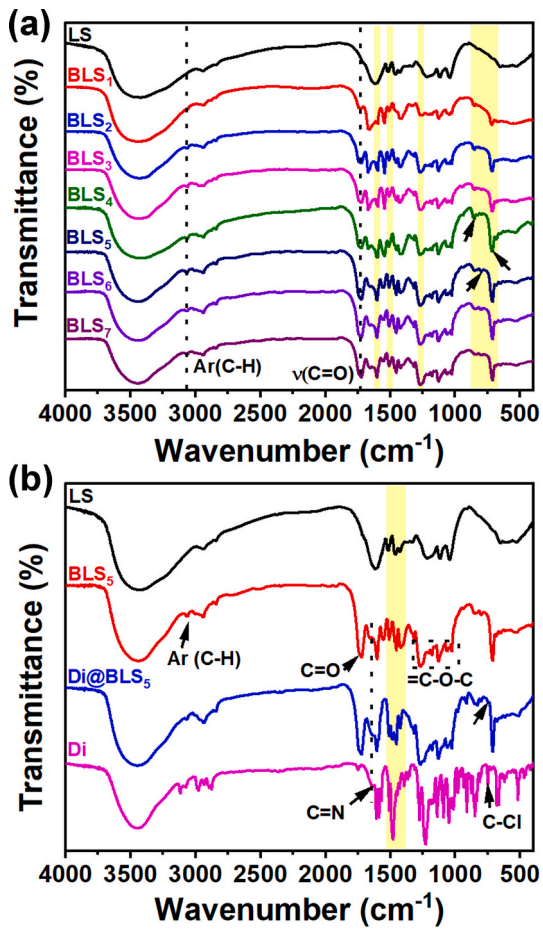

Fig. 1. FTIR spectra of (a) different benzoyloxylation lignin sulfonates (BLS_1, BLS_2, BLS_3, BLS_4, BLS_5, BLS_6, and BLS_7), LS and (b) BLS_5, $Di@BLS_5$, and Di.

purchased from Wuhan Yuancheng Technology Development Co., Ltd. (China). Sodium dodecylsulfate (SDS, 93 %) was obtained from Shandong Yousuo Chemical Technology Co., Ltd. (China). Lignin sulfonic acid sodium salt and benzoic anhydride (98 %) were purchased from Shanghai Dibai Chemicals Technology Co., Ltd. (China). Difenoconazole microemulsion (Di ME, 10 %) was purchased from Hebei Shangrui Chemical Technology Co., Ltd. (China).

2.2. Syntheses of benzoyloxylation lignin sulfonates

Lignin sulfonate (1 g) was added to 15 mL of dimethyl formamide (DMF) with 10 % LiCl and completely dissolved at 90 °C. Subsequently, 1, 2, 3, 4, 5, 6, or 7 g of benzoic anhydride and 1 equivalents of triethylamine (relative to benzoic anhydride) were added, respectively. The reaction was allowed to proceed at 60 °C under stirring and N_2 atmosphere. After reaction for 24 h, the mixture was precipitated into 300 mL of isopropanol and isolated by centrifugation (8000 rpm, 5 min). The different benzoyloxylation lignin sulfonates (code was BLS_1, BLS_2, BLS_3, BLS_4, BLS_5, BLS_6, and BLS_7) were obtained respectively after washing with isopropanol twice and drying at 40 °C in a vacuum oven.

2.3. Preparation of difenoconazole-loaded nanocarriers

The preparation of fungicide-loaded lignin nanoparticles was carried out by solvent exchange or solvent evaporation method according to the solubility of the different BLS products (Table S1). In the case of the solvent exchange method, 50 mg of BLS and 10 mg of difenoconazole (Di) were dissolved in 500 μL of dimethyl sulfoxide (DMSO). Then the solution was added into an aqueous solution (5 mL) with 0.2 % wt% of SDS under vigorous stirring for 5 min and ultrasonication for 15 min. The Di-loaded BLS nanoparticle (Di@BLS) was obtained after extensively dialyzed against distilled water for 24 h at room temperature (MWCO 3500). For the solvent evaporation method, BLS (50 mg) and Di (10 mg) were dissolved in 500 mg of dichloromethane (DCM), and then the solution was added into an aqueous solution (5 mL) with 0.2 % wt% of SDS. The resulting mixture was pre-emulsified with homogeneous shearing for 1 min (10,000 rpm), and then was submitted to ultrasonication for 1 min (1/2 in tip, 70 % amplitude, 1 s pulse on followed by 2 s pulse off). The remaining dichloromethane was further evaporated by vigorous magnetic stirring (1200 rpm) at room temperature, and the Di@BLS was obtained after washing.

2.4. Characterization

^{1}H nuclear magnetic resonance spectroscopy was performed using a Zhongke-Niujin WNMR-I spectrometer (China) at 400 MHz. FT-IR spectra were recorded in the range of 4000–400 cm^{-1} with 32 scans at a resolution of 2 cm^{-1} using FT-IR spectrometer (ThermoFisher, Nicolet Ava-tar 370, USA) at room temperature. The sulfur and carbon content were determined using an elemental analyzer (Elementar, Vario EL Cube, Germany). The morphology of the samples was observed by SEM (Zeiss, G300, Germany). The zeta potential and size distribution of the samples were determined through a Mastersizer ZS-90 laser diffraction particle size analyzer (Malvern, U.K.).

2.5. Formulation stability analysis

The stability of Di@BLS was analyzed using Turbiscan Lab Expert (Formulation, France) as a previous study [37]. The stability analysis for different Di@BLS and commercial difenoconazole microemulsion (Di ME) was performed as a variation of backscattering (ΔBS) profiles. Measurements were performed using a a2 near-infrared LED at a wavelength of 880 nm for 1 h. Experimental data were correlated in percentage to the light flux of two reference standards constituted by a polystyrene latex suspension (absence of transmission and maximum backscattering) and a silicon oil (maximum transmission and absence of backscattering). The turbiscan stability index (TSI) was calculated based on the variation in the backscattering light intensity at different locations of the test tube (top, middle, and bottom) as formula [38]:

$$TSI = \sum_i \frac{\sum_h |scan_i(h) - scan_{i-1}(h)|}{H}$$

where $scan_i(h)$ is the light intensity of the i-th scan at a height of h, and H is the total height of the measured sample.

2.6. Pesticide release property

The release property of Di from Di@BLS nanoparticles was conducted *via* suspending the same Di concentration (about 2000 μg/mL) of $Di@BLS_5$ and Di ME in 2.5 mL of deionized water and added into a dialysis bag (molecular weight cut off: 1 kDa), respectively. And then, the samples were dialyzed in 100 mL of deionized water with 1 % tween-80 under moderate shaking at 25 °C. At different intervals, 1 mL samples were taken out from the release medium, and the same volume of medium was added. The collected samples were determined by HPLC (Shimazu, LC-20A, Japan). A Shimadzu LC-20A HPLC system equipped with a diode array detector and a Shimadzu InertSustainR C18 column (4.6 × 250 mm, 5 μm particle size) was used for HPLC analysis. The mobile phase consisted of water and acetonitrile (32:68, v/v) flowing at a rate of 1 mL/min. The analysis was performed at 240 nm. The amount of difenoconazole release was calculated using the standard calibration curve, which formed from different concentrations of difenoconazole acetonitrile solution. The cumulative release percentage of

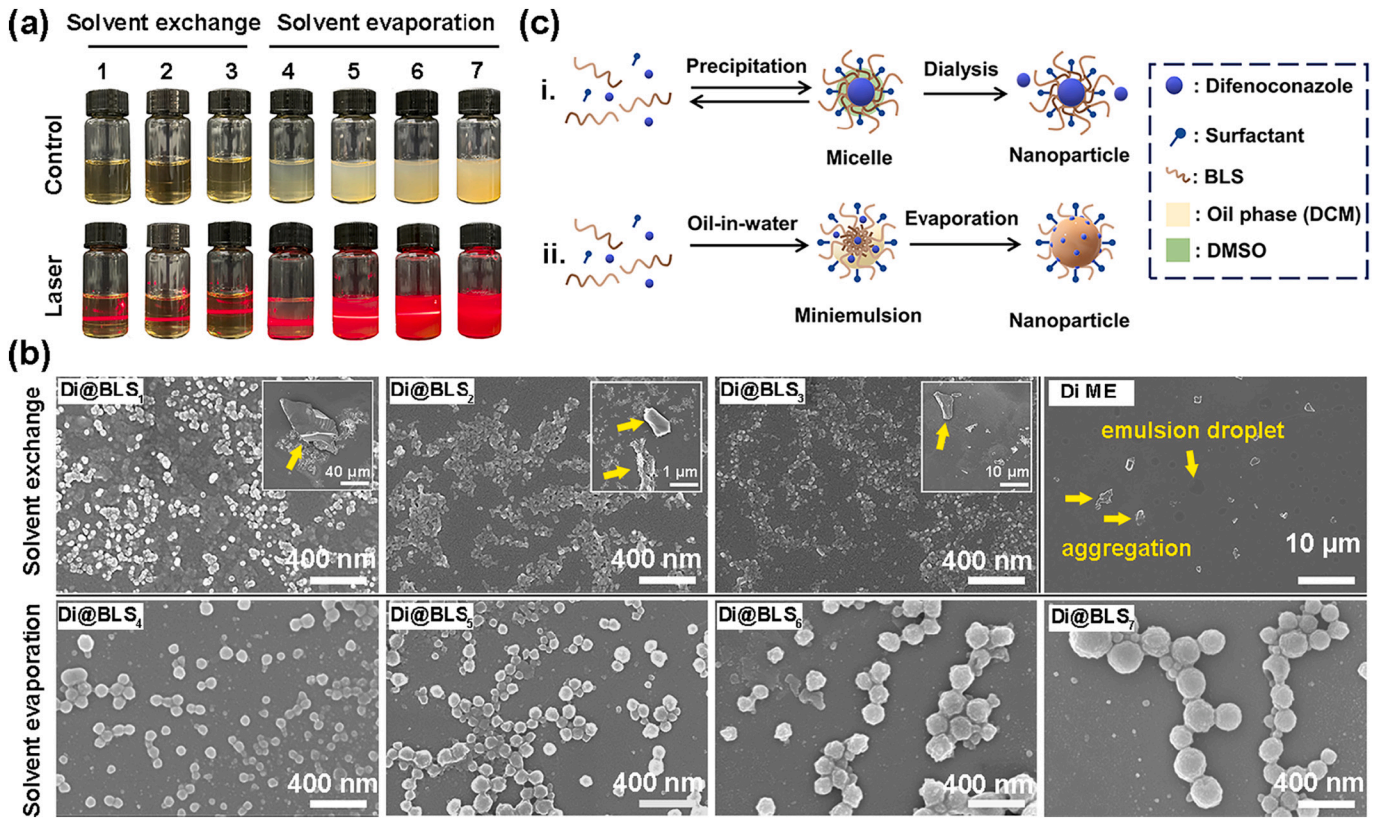

Fig. 2. (a) Photographs of different Di@BLS formulations with the same Di concentration under laser radiation (samples 1, 2, 3, 4, 5, 6, and 7 represent Di@BLS_1, Di@BLS_2, Di@BLS_3, Di@BLS_4, Di@BLS_5, Di@BLS_6, and Di@BLS_7). (b) SEM images of different Di@BLS nanoparticles obtained by solvent exchange or solvent evaporation method, and SEM images of Di ME. (c) Schematic of the preparation of Di@BLS nanoparticles using (i) solvent exchange or (ii) solvent evaporation method. Different Di@BLS means the Di@BLS nanoparticles obtained by solvent exchange or solvent evaporation method using the BLS with varying ratios of reaction.

difenoconazole was calculated using the following equation:

$$\text{Cumulative release } (\%) = \sum_{t=0}^{t} \frac{M_t}{M_0} \times 100\%$$

where M_t is the amount of Di released to each sampling time point, t is the time of the release of Di-loaded and M_0 is the initial weight of the Di-loaded in the BLS nanoparticles.

2.7. Light stability analysis

The photostability of the samples was determined by exposing them to UV light (254 nm). Briefly, the same Di concentration of Di@BLS_5 and Di ME were divided into qual aliquots of 1 mL and placed into centrifuge tubes, respectively, and then were irradiated by UV light (254 nm, 6 W). The distance of the light source from the suspension surface was 10 cm. Periodically, a tube was selected for HPLC analysis to determine the remaining concentration of Di. Each experiment was repeated three times.

2.8. In vitro bioactivity assay

The effective concentration at which the mycelial growth rate was inhibited by 50 % (EC_{50}) of Di@BLS_5 against fungi was investigated using the growth-inhibition assay on potato dextrose agar (PDA) plates. The *Colletotrichum gloeosporioides* (provided by Chuanqing Zhang, Zhejiang A&F University) was used as a model fungus for the bioactivity assay. Briefly, mycelial plugs of the fungus were grown in the center of PDA plates, which were treated with different concentrations of Di@BLS_5, Di ME, and Di technical (Di Tech). The final Di concentrations were 0.0625, 0.25, 0.5, 1 and 4 μg/mL respectively. The plates were cultured at 25 °C for 5 days. The EC_{50} values were calculated by linear regression analysis of a colony diameter on log-transformed fungicide concentrations. Each experiment was repeated three times.

2.9. In vivo control efficacy assay in pot experiment

About 2-month-old strawberry plants (cultivar Arena) were sprayed with Di ME and Di@BLS_5 at a Di concentration of 100 mg/L with hand-held sprayer. The plants were challenged with *Colletotrichum gloeosporioides* by artificial inoculation at day 0, 7, or 14 after the spray treatments, and then incubated in the green house. The detailed method was according to the previous report [15]. Lesion diameters were measured in two perpendicular directions 7 days post the fungal challenge. The BLS_5 carrier and water were as the controls. Each experiment was repeated five times. The concentration of BLS_5 was the same as that of the carrier of the Di@BLS_5. Control efficacy was calculated by the following equation:

$$\text{Control efficacy } (\%) = \frac{D_0 - D}{D_0} \times 100\%$$

where the D_0 is the lesion diameter in the control, and D is the lesion diameter in the treatment.

2.10. Foliar retention and distribution investigation

The retention of Di on the surface of leaves was measured according to the previous literature with minor modification [39]. Briefly, 1 mL of the same Di concentration (100 μg/mL) of Di@BLS_5 or Di ME was

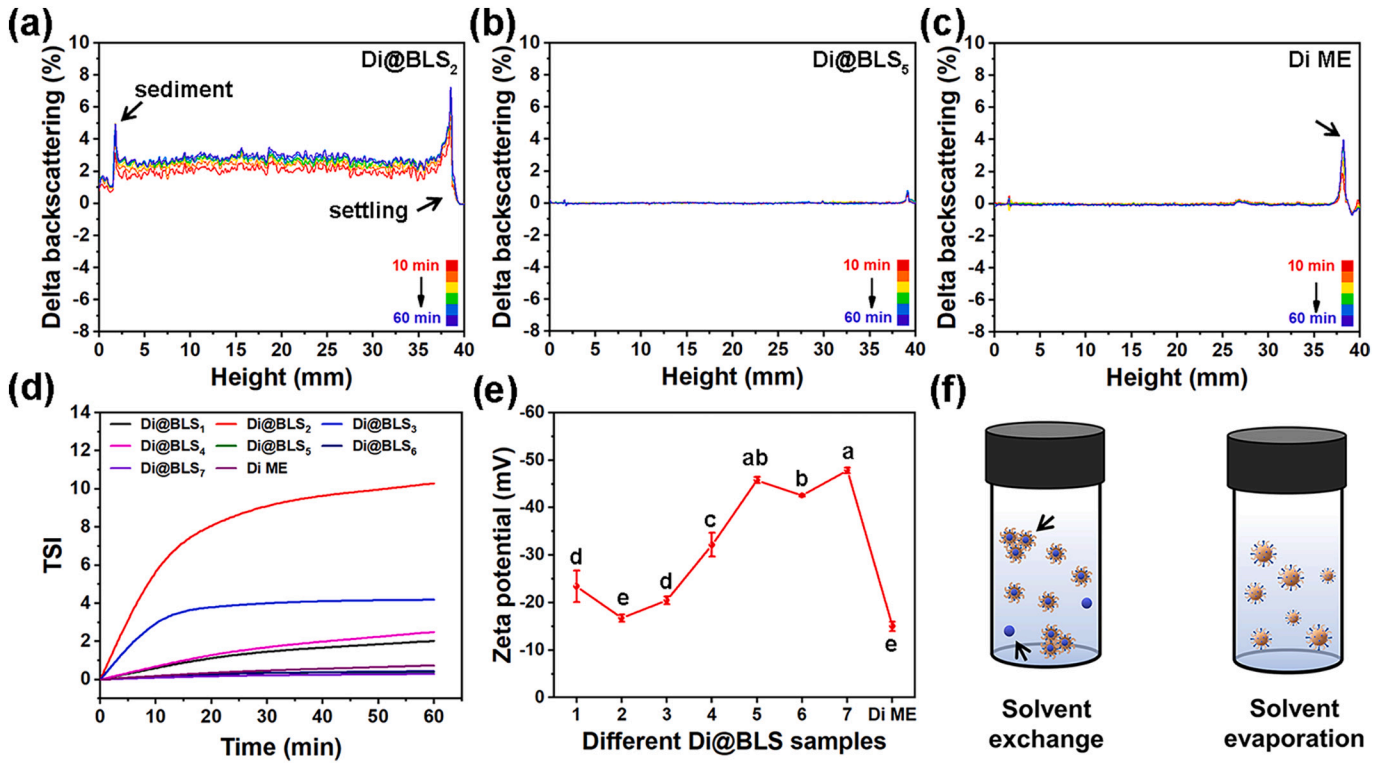

Fig. 3. Backscattering profiles of (a) Di@BLS_2 prepared using solvent exchange method, (b) Di@BLS_5 prepared using solvent evaporation, and (c) Di ME. Turbiscan stability index (TSI) values of (d) different Di@BLS nanoparticle and Di ME. (e) Zeta potential of different Di@BLS nanoparticle and Di ME. (f) Schematic illustration of the formulation stability.

sprayed evenly onto the peanut or cucumber leaves, which were then tilted at an angle of 45° relative to the ground. After air-drying for 2 h, the halves of leaf were sprayed with 10 mL of deionized water as a simulation of rain wash. Subsequently, the region of the treated leaf (5 × 5 mm) was randomly selected after air-drying again, and the Di was extracted for detection by HPLC. The distribution of samples on the surface of leaves was observed using SEM. Each experiment was repeated three times.

2.11. Statistical analysis

For multiple group comparisons, one-way ANOVA followed by a Duncan test was used for analysis *via* Statistical Product and Service Solutions (SPSS). Marking different letter or asterisk (*) is considered as significant difference at $P < 0.05$.

3. Results and discussion

3.1. Synthesis and characterization

Lignin sulfonate was esterified with different benzoic acid to regulate the hydrophilicity of lignin sulfonate. After esterification, the water solubility of the lignin sulfonates decreased because as the number of hydroxyl groups were reduced. Elemental analysis (Table S1) showed that as the degree of substitution of benzoic acid increased, the content of sulfur elements in the products showed a decreasing trend (from 1.26 mmol/g to 0.50 mmol/g). Conversely, the content of carbon elements gradually increased. Until the reaction ratio of 1:5 (mass ratio of lignin sulfonate to benzoic anhydride), the carbon element content tends to equilibrium, indicating that most of the active hydroxyl groups in lignin sulfonate had been esterified. The successful functionalization with benzoic acid was proven by ^{1}H NMR (Fig. S1). It showed the resonances from 7.2 to 8.2 ppm corresponding to the protons of the aromatic ring of benzoic ether.

FTIR spectroscopy further proved the successful modification of lignin sulfonate by the enhanced peak (3066, 1600, and 1500 cm^{-1}) or additional peak at 1730 cm^{-1}, which correspond to the C—H and skeleton vibration of benzoic group, and C═O respectively (Fig. 1a). With the increase of the degree of substitution, the relative intensity of these characteristic peaks increased. The additional peaks from 900 to 600 cm^{-1} were attributed to characteristic vibrations of benzene ring. Compared with LS, BLS_1, BLS_2, BLS_3 and BLS_4 had two characteristic peaks at 857 cm^{-1} and 718 cm^{-1}, which belong to the benzene ring skeleton vibration of monosubstituted benzoic acid. The relative strength of the peak also increased with the increase of the degree of substitution. However, in addition to these two peaks, a new peak at 797 cm^{-1} appeared in BLS_5, BLS_6 and BLS_7, indicating that the less reactive phenolic hydroxyl groups in LS were also involved in esterification. For the fungicide-loaded lignin nanocarriers (difenoconazole, Di) additional characteristic vibrations of Di such as C═N and C—Cl were detected in the IR spectra (Fig. 1b) [40].

As shown in the appearance of different Di@BLS formulation with the same Di concentration (Fig. 2a), the formulation prepared by the solvent exchange method tends to be as transparent as microemulsions, and a clear light path can be formed under laser irradiation. However, with the increase of the degree of substitution of benzoic acid, the prepared formulation gradually became turbid, and the scattering of light was also becoming more severe. It can be inferred that the fungicide formulation with different particles size can be obtained using different BLS and preparation methods. SEM was further used to explore the morphology of fungicide-loaded nanoparticles. As shown in Figs. 2b and S3, the size of Di@BLS_1, Di@BLS_2, and Di@BLS_3 prepared by solvent exchange method was about 32 ± 5, 31 ± 5, and 26 ± 4 nm. Although the nanoparticles prepared by the solvent exchange were small, other crystal particles with micron-scale can be observed. As for using the solvent evaporation method, the size of Di@BLS_4, Di@BLS_5, Di@BLS_6, and Di@BLS_7 was about 83 ± 12, 92 ± 21, 131 ± 26, and 137 ± 29 nm calculated by randomly sampling at least 200 nanoparticles from SEM

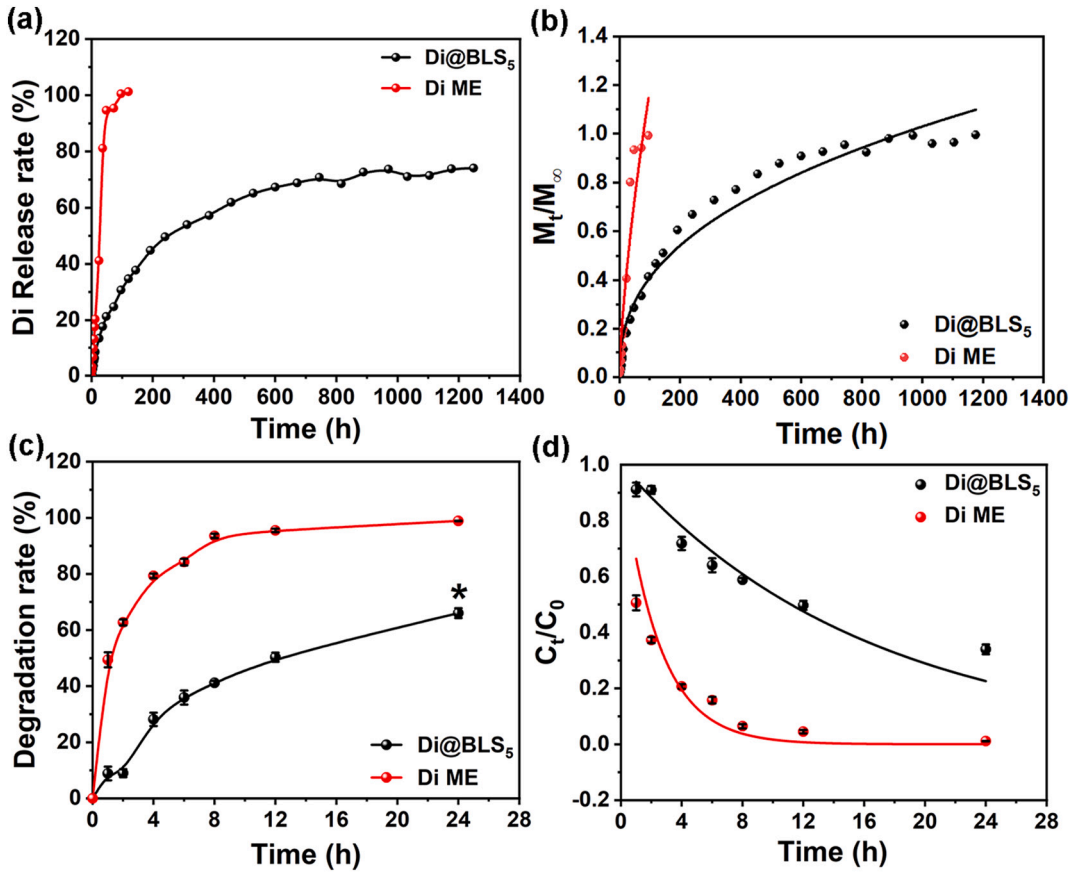

Fig. 4. (a) Cumulative release profile, and (b) fitting curves of Ritger-Peppas model of Di@BLS_5 and Di ME. (c) Degradation rate, and (d) first-order function kinetics of Di@BLS_5 and Di ME under ultraviolet light irradiation.

image, showing a trend of gradual increase, and no large crystal particles were observed in SEM. The reason for this result may be that the Di precipitated into the aqueous phase with the exchange of DMSO and water during dialysis. Conversely, due to the separation of oil (DCM) and water phase, hydrophobic Di could not enter the aqueous phase through the solvent exchange to not cause crystallization (Fig. 2c). Additionally, commercial difenoconazole microemulsion (Di ME), as a pesticide formulation with nanoscale, can be only observed the traces of emulsion droplets and many crystal particles with microns scale through SEM, but no solid nanoparticles (Fig. 2b). It proved that the micelles of pesticide with nano-size were only in water, which would make the size of pesticide change in some cases, such as after drying.

3.2. Formulation stability analysis

Turbiscan analysis can provide information on the destabilization process, and it can discriminate between particle migration (creaming or sedimentation) and particle size variation (flocculation or coalescence). Figs. 3a, b, c, and S3 showed delta backscattering (%) as a function of sample height (0–40 mm) and time (0−1 h) at 25 °C for different Di@BLS formulations with the same Di concentration and Di ME, respectively. The aggregation and migration of Di@BLS_5, Di@BLS_6, and Di@BLS_7 were thought to have not occurred because the backscattering profile was within the interval ± 2 % [41], indicating that it had high formulation stability, even more stable compared with Di ME in the short term. Conversely, the backscattering profile of Di@BLS_1, Di@BLS_2, Di@BLS_3, and Di@BLS_4 had a large range of variation, especially at the top of the formulation, showing that the particles were settling. The instability of the Di@BLS formulation can also be reflected by the TSI value (Figs. 3d and S4). A higher TSI value indicated a less stable formulation sample [42]. Besides, zeta potential showed that the nanoparticles prepared by solvent evaporation method had a higher negative charge than those prepared by solvent exchange method (Fig. 3e). Hence, combined with the results of SEM, it could be inferred that the reason for the poor stability of Di@BLS formulation was the small size of particles with a low negative charge on the surface, which led to the aggregation of the particles or the crystallization of fungicides in the aqueous phase (Fig. 3f). According to the complexity of preparation, cost and stability, the Di@BLS_5 was finally selected as the best formulation for subsequent evaluation of other properties.

3.3. Fungicide release and light stability

The slow release of fungicide may be one of the effective ways to improve the duration of the fungicide in agricultural production. Fig. 4a showed the release behavior of the Di@BLS_5 and Di ME formulations in an aqueous solution containing 1 % of the non-ionic surfactant Tween-80. Di ME exhibited rapid release in the initial stage. The cumulative release rate of the Di ME reached 95 % at 48 h and 100 % at 96 h. Whereas the release rate of Di@BLS_5 showed a very slow increasing trend and significantly slower than that of Di ME, indicating that encapsulation delayed the release. After 1248 h, the cumulative release rate of Di@BLS_5 was 74 %.

To further investigate the release profile of the Di@BLS_5, some classical models, known as the zero-order model, first-order model, Higuchi model, and Ritger-Peppas model were used [43,44]. Detailed formulas are shown in the Supporting Information. As shown in Figs. 4b, S6 and Table S2, the release profile of Di@BLS_5 had the highest R^2 (0.969) when calculated using the Ritger-Peppas model, and the diffusion exponent was 0.397, indicating that the release of Di from the BLS_5 carrier followed the Fickian diffusion. While the release of Di ME is more consistent with the first-order model with the R^2 of 0.961, showing that

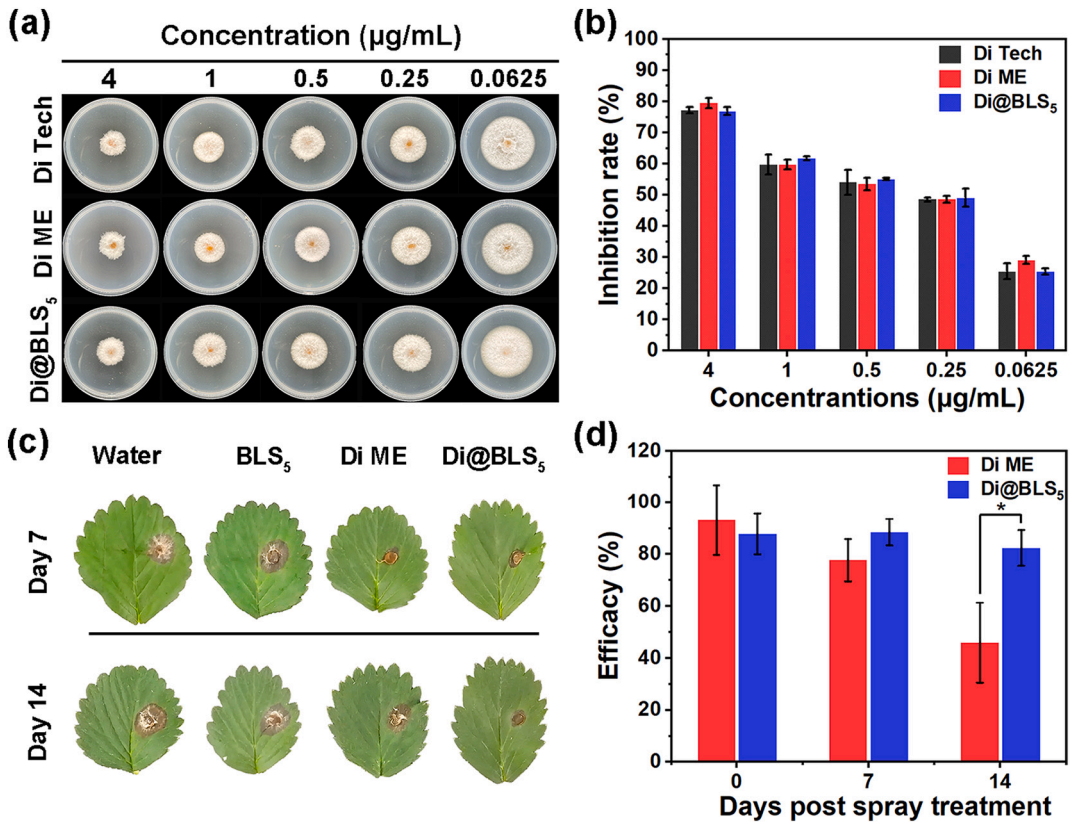

Fig. 5. (a) Photographs and (b) antimicrobial activities of Di Tech, Di ME and Di@BLS_5 against *Colletotrichum gloeosporioides*. (c) Photographs and (d) control efficacy of Di ME and Di@BLS_5 against *Colletotrichum gloeosporioides* in pot experiments on strawberry leaves.

the release of Di from Di ME is dependent only on concentration. Hence, BLS_5 carrier had a better control effect on the release rate of fungicide compare the commercial formulation.

The instability of pesticide to UV light is also one of the critical factors affecting the duration of pesticide efficacy [45]. As shown in Fig. 4c, the degradation rate of Di ME reached 80 % and was almost complete after 4 h and 24 h of UV radiation (254 nm). However, the decomposition rate of Di in BLS_5 nanoparticles was only 28 % and 66 % after being exposed to UV light for the same time. The degradation half-lives of two difenoconazole formulation under the UV light irradiation was determined following first-order function kinetics with the formulas:

$$C_t = C_0 e^{-kt}$$

$$t_{1/2} = \frac{ln2}{k}$$

where C_t is the concentration of the fungicide at time t (mg/L), C_0 denotes the initial concentration of the fungicide (mg/L), k is the rate constant of degradation (h^{-1}), and $t_{1/2}$ is the degradation half-life of the fungicide [46]. The degradation kinetics and $t_{1/2}$ of Di@BLS_5 and Di ME were shown in Table S3. The $t_{1/2}$ of Di@BLS_5 was 11.18 h under the UV light irradiation, while Di ME was only 1.69 h, indicating that BLS_5 nanocarrier could effectively protect the fungicide from UV degradation. The excellent anti-photolysis property of Di@BLS_5 was contributed to the presence of partially unreacted phenolic hydroxyl groups in the BLS_5 nanocarriers, and the fungicide-inside structure of nanoparticle which behaved as a shield to protect Di from UV light [47]. These results exhibited that the BLS_5 nanocarrier could improve the leaching time and light stability of Di, which could favor prolonging the duration and improving the utilization efficiency of Di, thus being beneficial to extend the fungicide efficacy period, especially for crops with long growth cycles, and reduce environmental pollution and crop pesticide high residues risk caused by multiple pesticide sprays during disease outbreak cycles.

3.4. *In vitro* bioactivity

The fungicidal activities of Di Tech, Di ME, and Di@BLS_5 with different Di concentrations against *Colletotrichum gloeosporioides* (*C. gloeosporioides*) are shown in Fig. 5a, b. The fungicidal activities of all the three samples depended on the concentration, and the high concentration of BLS_5 nanoparticles (20 μg/mL) had no fungicidal activity (Fig. S7). Besides, the EC_{50} values of Di Tech, Di ME and Di@BLS_5 were further calculated using the percent inhibition of mycelial growth (Table S4), and values were 0.40, 0.34, and 0.36 μg/mL, respectively. The results indicated that the loaded difenoconazole still had fungicidal activity that was not significantly different from that of the commercial Di microemulsion.

3.5. *Fungicidal activity in pot experiment*

The fungicidal activity of Di@BLS_5 nanoparticles against *C. gloeosporioides* was further verified on strawberry leaves (Fig. 5c, d). The results showed that the efficacy of Di ME and Di@BLS_5 was not significantly different when the plants were challenged by the fungus at 0 days or 7 days post spraying. However, the efficacy of Di ME treatment was reduced to 46 ± 15 % for the fungal infection 14 days after spraying, whereas the efficacy of Di@BLS_5 treatment was still relatively high (82 ± 7 %) and was not significantly reduced compared with the treatment at 7 days post spraying. The high duration of Di@BLS_5 could be attributed to the BLS_5 carrier which could protect the active ingredients from premature degradation, slowly release and improve the retention of the fungicide. Conversely, the naked Di ME certainly would not provide long

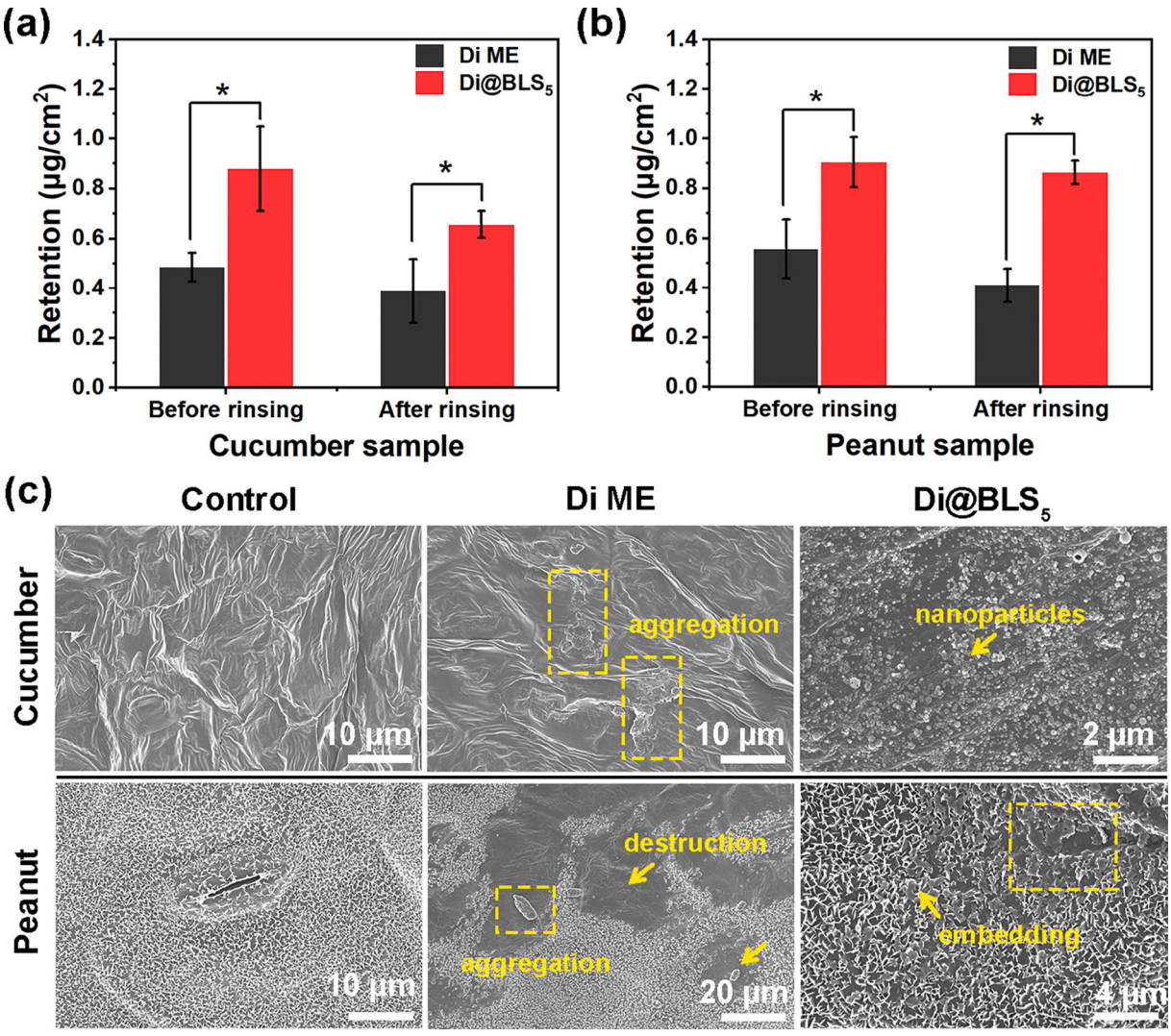

Fig. 6. Leaf retention of Di ME and Di@BLS_5 on the surface of (a) cucumber or (b) peanut leaves before and after rinsing with water. (c) SEM images of cucumber and peanut foliage surface treated with same Di concentration of Di ME and Di@BLS_5.

protection for plants under environmental conditions because its instability to light, microorganism, enzyme or other factors.

3.6. Foliar retention and distribution

After the pesticide spraying onto crops, the distribution and retention on crop leaf surface play a decisive role in the effective use of pesticide. Hence, the folia retention before and after rinsing with water was measured to evaluate the affinity of Di@BLS_5 drops on leaves. As shown in Fig. 6a and b, the Di retention of Di@BLS_5 on the more hydrophilic cucumber leaves before and after rinsing with water was 1.81 and 1.69 times greater than that of Di ME, respectively. As for the hydrophobic peanut leaves, the Di retention of Di@BLS_5 was also 1.63 and 2.11 times higher than that of Di ME before and after rinsing with water, respectively. Besides, compared with cucumber, the Di retention rate of Di@BLS_5 was higher than Di ME after spraying onto peanuts (Fig. S8), indicating that Di@BLS_5 had the better anti-scour ability on peanut leaves surface. SEM further revealed the reason for the results. Fig. 6c showed that the Di@BLS_5 nanoparticles could be evenly distributed on the cucumber and peanut foliage surface. However, although Di ME existed in the water phase at the nanoscale, the distribution of nanoparticles could not be found after spraying on the leaves of plants. Instead, it agglomerated into large particles, resulting in uneven distribution. Additionally, it was also observed that the structure of the waxy layer on peanut leaves was destroyed, possibly due to the presence of a large amount of surfactant in Di ME, which might increase the risk of pathogens infecting crops [48]. Notably, Di@BLS_5 nanoparticles were observed to be embedded between gaps of waxy structure on the surface of peanut leaves, which explained why Di@BLS_5 had a better ability to resist scour in peanut leaves. Consequently, the increased Di retention of Di@BLS_5 maybe because of the even distribution of nanoparticles on the leaves surface, or the topological structure was formed between the wax layer and Di@BLS_5 nanoparticles [49].

4. Conclusion

In this study, a fungicide-loaded nanoparticle formulation constructed by benzoyloxylation lignin sulfonates using a solvent exchange or solvent evaporation method was reported the first time. The nanoparticles obtained by solvent evaporation using a 1:5 reaction mass ratio (lignin sulfonate: benzoic anhydride) of benzoyloxylation lignin sulfonate were finally determined through a series of characterization as the optimal formulation. The optimal formulation showed better duration, photostability, efficacy, and foliar retention compared with commercial fungicide microemulsions. Although this formulation had the advantages of environmental friendliness, water-based, no organic solvents,

and fewer surfactants compared with commercial pesticide formulation, the risk of pollution due to this technology of nano-formulation also should be considered. Furthermore, it was also worthwhile to explore the direction of this study on how to rationalize the scaled-up production and improve the pesticide content. Overall, this study provided a promising approach for developing green and environmentally friendly nanopesticide formulations and the development of sustainable agriculture.

CRediT authorship contribution statement

W. Liang: Conceptualization, Formal analysis, Methodology, Investigation, Writing - Original draft. **J. Zhang:** Investigation, Data curation, Writing - Original draft. **F. R. Wurm:** Conceptualization, Writing - Review & editing. **R. Wang:** Funding acquisition. **J. Cheng:** Validation, Writing - review & Editing. **Z. Xie:** Investigation. **X. Li:** Project administration, Writing - Review & editing. **J. Zhao:** Project administration, Resources, Funding acquisition, Supervision.

Declaration of competing interest

The authors declare that they have no known competing financial interests or personal relationships that could have appeared to influence the work reported in this paper.

Acknowledgements

This work was financially supported by the National Natural Science Foundation of China (No. 31872022), the Public Welfare Technology Application Research Project of Zhejiang Province Analysis and Testing Project (No. LGC22C140001), and The Science and Technology Project of Zhejiang Province (No. 2021C02045 and 2021C02010). Thanks to the research group of Chuanqing Zhang at Zhejiang A&F University for their help on the *Colletotrichum gloeosporioides*.

Appendix A. Supplementary data

Supplementary data to this article can be found online at https://doi.org/10.1016/j.ijbiomac.2022.08.103.

References

[1] E. Crist, C. Mora, R. Engelman, The interaction of human population, food production, and biodiversity protection, Science 356 (6335) (2017) 260–264.
[2] J. Clay, Freeze the footprint of food, Nature 475 (7356) (2011) 287–289.
[3] C.A. Damalas, I.G. Eleftherohorinos, Pesticide exposure, safety issues, and risk assessment indicators, Int. J. Environ. Res. Public Health 8 (5) (2011) 1402–1419.
[4] V. Kumar, P. Kumar, Pesticides in agriculture and environment: impacts on human health, in: Contaminants in Agriculture and Environment: Health Risks and Remediation 1, 2019, p. 76.
[5] B. Gevao, K.T. Semple, K.C. Jones, Bound pesticide residues in soils: a review, Environ. Pollut. 108 (1) (2000) 3–14.
[6] N.F. Wan, X.Y. Ji, J.X. Jiang, X. Deng, K.H. Huang, B. Li, An eco-engineering assessment index for chemical pesticide pollution management strategies to complex agro-ecosystems, Ecol. Eng. 52 (2013) 203–210.
[7] M.N. Naqqash, A. Gökçe, A. Bakhsh, M. Salim, Insecticide resistance and its molecular basis in urban insect pests, Parasitol. Res. 115 (4) (2016) 1363–1373.
[8] S. Engelskirchen, R. Maurer, T. Levy, R. Berghaus, H. Auweter, O. Glatter, Highly concentrated emulsified microemulsions as solvent-free plant protection formulations, J. Colloid Interface Sci. 388 (2012) 151–161.
[9] W.L. Liang, A.X. Yu, G.D. Wang, F. Zheng, P.T. Hu, J.L. Jia, H.H. Xu, A novel water-based chitosan-La pesticide nanocarrier enhancing defense responses in rice (Oryza sativa L.) growth, Carbohydr. Polym. 199 (2018) 437–444.
[10] C. Bartolucci, A. Antonacci, F. Arduini, D. Moscone, L. Fraceto, E. Campos, R. Attaallah, A. Amine, C. Zanardi, L.M. Cubillana-Aguilera, J.M.P. Santander, V. Scognamiglio, Green nanomaterials fostering agrifood sustainability, TrAC Trends Anal. Chem. 125 (2020), 115840.
[11] M.A. Hamburg, FDA's approach to regulation of products of nanotechnology, Science 336 (6079) (2012) 299–300.
[12] X. Zhao, H.X. Cui, Y. Wang, C.J. Sun, B. Cui, Z.H. Zeng, Development strategies and prospects of nano-based smart pesticide formulation, J. Agric. Food Chem. 66 (26) (2018) 6504–6512.
[13] T.O. Machado, J. Grabow, C. Sayer, P.H. de Araújo, M.L. Ehrenhard, F.R. Wurm, Biopolymer-based nanocarriers for sustained release of agrochemicals: a review on materials and social science perspectives for a sustainable future of agri-and horticulture, Adv. Colloid Interface Sci. 303 (2022), 102645.
[14] W. Liang, J. Cheng, J. Zhang, Q. Xiong, M. Jin, J. Zhao, pH-responsive on-demand alkaloids release from core-shell ZnO@ZIF-8 nanosphere for synergistic control of bacterial wilt disease, ACS Nano 16 (2) (2022) 2762–2773.
[15] W.L. Liang, Z.G. Xie, J.L. Cheng, D.X. Xiao, Q.Y. Xiong, Q.W. Wang, J.H. Zhao, W. J. Gui, A light-triggered pH-responsive metal-organic framework for smart delivery of fungicide to control sclerotinia diseases of oilseed rape, ACS Nano 15 (4) (2021) 6987–6997.
[16] D.X. Xiao, J.L. Cheng, W.L. Liang, L.L. Sun, J.H. Zhao, Metal-phenolic coated and prochloraz-loaded calcium carbonate carriers with pH responsiveness for environmentally-safe fungicide delivery, Chem. Eng. J. 418 (2021), 129274.
[17] G.D. Wang, Y.Y. Xiao, H.H. Xu, P.T. Hu, W.L. Liang, L.J. Xie, J.L. Jia, Development of multifunctional avermectin poly(succinimide) nanoparticles to improve bioactivity and transportation in rice, J. Agric. Food Chem. 66 (43) (2018) 11244–11253.
[18] W.L. Liang, A.X. Yu, G.D. Wang, F. Zheng, J.L. Jia, H.H. Xu, Chitosan-based nanoparticles of avermectin to control pine wood nematodes, Int. J. Biol. Macromol. 112 (2018) 258–263.
[19] D. Xiao, W. Liang, Z. Xie, J. Cheng, Y. Du, J. Zhao, A temperature-responsive release cellulose-based microcapsule loaded with chlorpyrifos for sustainable pest control, J. Hazard. Mater. 403 (2021), 123654.
[20] S.J. Beckers, L. Wetherbee, J. Fischer, F.R. Wurm, Fungicide-loaded and biodegradable xylan-based nanocarriers, Biopolymers 111 (12) (2020), e23413.
[21] M. Auffan, J. Rose, J.-Y. Bottero, G.V. Lowry, J.-P. Jolivet, M.R. Wiesner, Towards a definition of inorganic nanoparticles from an environmental, health and safety perspective, Nat. Nanotechnol. 4 (10) (2009) 634–641.
[22] N. Phogat, S.A. Khan, S. Shankar, A.A. Ansary, I. Uddin, Fate of inorganic nanoparticles in agriculture, Adv. Mater. Lett. 7 (1) (2016) 03–12.
[23] M. Kumar, X. Xiong, M. He, D.C.W. Tsang, J. Gupta, E. Khan, S. Harrad, D. Hou, Y. S. Ok, N.S. Bolan, Microplastics as pollutants in agricultural soils, Environ. Pollut. 265 (2020), 114980.
[24] V.K. Thakur, M.K. Thakur, Recent advances in graft copolymerization and applications of chitosan: a review, ACS Sustain. Chem. Eng. 2 (12) (2014) 2637–2652.
[25] X.P. Shen, J.L. Shamshina, P. Berton, G. Gurau, R.D. Rogers, Hydrogels based on cellulose and chitin: fabrication, properties, and applications, Green Chem. 18 (1) (2016) 53–75.
[26] P. Jedrzejczak, M.N. Collins, T. Jesionowski, L. Klapiszewski, The role of lignin and lignin-based materials in sustainable construction-a comprehensive review, Int. J. Biol. Macromol. 187 (2021) 624–650.
[27] M. Culebras, M. Pishnamazi, G.M. Walker, M.N. Collins, Facile tailoring of structures for controlled release of paracetamol from sustainable lignin derived platforms, Molecules 26 (6) (2021) 1593.
[28] M. Culebras, A. Barrett, M. Pishnamazi, G.M. Walker, M.N. Collins, Wood-derived hydrogels as a platform for drug-release systems, ACS Sustain. Chem. Eng. 9 (6) (2021) 2515–2522.
[29] A. Beaucamp, M. Culebras, M.N. Collins, Sustainable mesoporous carbon nanostructures derived from lignin for early detection of glucose, Green Chem. 23 (15) (2021) 5696–5705.
[30] U.M. Ahmad, N. Ji, H. Li, Q. Wu, C. Song, Q. Liu, D. Ma, X. Lu, Can lignin be transformed into agrochemicals? Recent advances in the agricultural applications of lignin, Ind. Crop. Prod. 170 (2021), 113646.
[31] J. Luo, D.-X. Zhang, T. Jing, G. Liu, H. Cao, B.-X. Li, Y. Hou, F. Liu, Pyraclostrobin loaded lignin-modified nanocapsules: delivery efficiency enhancement in soil improved control efficacy on tomato fusarium crown and root rot, Chem. Eng. J. 394 (2020), 124854.
[32] D.X. Zhang, G. Liu, T.F. Jing, J. Luo, G. Wei, W. Mu, F. Liu, Lignin-modified electronegative epoxy resin nanocarriers effectively deliver pesticides against plant root-knot nematodes (Meloidogyne incognita), J. Agric. Food Chem. 68 (47) (2020) 13562–13572.
[33] Y. Li, D. Yang, S. Lu, S. Lao, X. Qiu, Modified lignin with anionic surfactant and its application in controlled release of avermectin, J. Agric. Food Chem. 66 (13) (2018) 3457–3464.
[34] S.J. Beckers, I.A. Dallo, I. Del Campo, C. Rosenauer, K. Klein, F.R. Wurm, From compost to colloids—valorization of spent mushroom substrate, ACS Sustain. Chem. Eng. 7 (7) (2019) 6991–6998.
[35] S. Shu, C. Sun, X. Zhang, Z. Wu, Z. Wang, C. Li, Hollow and degradable polyelectrolyte nanocapsules for protein drug delivery, Acta Biomater. 6 (1) (2010) 210–217.
[36] C. Allen, D. Maysinger, A. Eisenberg, Nano-engineering block copolymer aggregates for drug delivery, Colloids Surf. B: Biointerfaces 16 (1–4) (1999) 3–27.
[37] D. Xiao, J. Cheng, W. Liang, C. Cheng, Q. Wang, R. Chai, Z. Yan, Y. Du, J. Zhao, Innovative approach to nano thiazole-zn with promising physicochemical and bioactive properties by nanoreactor construction, J. Agric. Food Chem. 67 (42) (2019) 11577–11583.
[38] K. Wang, G. Li, B. Zhang, Opposite results of emulsion stability evaluated by the TSI and the phase separation proportion, Colloids Surf. A Physicochem. Eng. Asp. 558 (2018) 402–409.
[39] D.X. Xiao, W.L. Liang, Z.S. Li, J.L. Cheng, Y.J. Du, J.H. Zhao, High foliar affinity cellulose for the preparation of efficient and safe fipronil formulation, J. Hazard. Mater. 384 (2020), 121408.

[40] Y. Wang, C. Li, Y. Wang, Y. Zhang, X. Li, Compound pesticide controlled release system based on the mixture of poly(butylene succinate) and PLA, J. Microencapsul. 35 (5) (2018) 494–503.
[41] C. Celia, E. Trapasso, D. Cosco, D. Paolino, M. Fresta, Turbiscan Lab® expert analysis of the stability of ethosomes® and ultradeformable liposomes containing a bilayer fluidizing agent, Colloids Surf. B: Biointerfaces 72 (1) (2009) 155–160.
[42] X. Zhao, G. Yu, J. Li, Y. Feng, L. Zhang, Y. Peng, Y. Tang, L. Wang, Eco-friendly Pickering emulsion stabilized by silica nanoparticles dispersed with high-molecular-weight amphiphilic alginate derivatives, ACS Sustain. Chem. Eng. 6 (3) (2018) 4105–4114.
[43] J. Dredan, I. Antal, I. Racz, Evaluation of mathematical models describing drug release from lipophilic matrices, Int. J. Pharm. 145 (1–2) (1996) 61–64.
[44] P.L. Ritger, N.A. Peppas, A simple equation for description of solute release II. Fickian and anomalous release from swellable devices, J. Control. Release 5 (1) (1987) 37–42.
[45] G. Tang, Y. Tian, J. Niu, J. Tang, J. Yang, Y. Gao, X. Chen, X. Li, H. Wang, Y. Cao, Development of carrier-free self-assembled nanoparticles based on fenhexamid and polyhexamethylene biguanide for sustainable plant disease management, Green Chem. 23 (6) (2021) 2531–2540.
[46] Y. Fu, X. Dou, Q. Lu, J. Qin, J. Luo, M. Yang, Comprehensive assessment for the residual characteristics and degradation kinetics of pesticides in panax notoginseng and planting soil, Sci. Total Environ. 714 (2020), 136718.
[47] Y.X. Li, M.S. Zhou, Y.X. Pang, X.Q. Qiu, Lignin-based microsphere: preparation and performance on encapsulating the pesticide avermectin, ACS Sustain. Chem. Eng. 5 (4) (2017) 3321–3328.
[48] J.T. Martin, Role of the cucticle in the defence against plant disease, Annu. Rev. Phytopathol. 2 (1) (1965) 81–100.
[49] K. Zhao, J. Hu, Y. Ma, T. Wu, Y. Gao, F. Du, Topology-regulated pesticide retention on plant leaves through concave janus carriers, ACS Sustain. Chem. Eng. 7 (15) (2019) 13148–13156.